



Short Communication

Application of friction surfacing for solid state additive manufacturing of cylindrical shell structures

Zina Kallien^{a,*}, Lars Rath^a, Arne Roos^a, Benjamin Klusemann^{a,b}

^a Helmholtz-Zentrum Hereon, Institute of Materials Mechanics, Solid State Materials Processing, Max-Planck-Straße 1, 21502 Geesthacht, Germany

^b Leuphana University Lüneburg, Institute for Production Technology and Systems, Universitätsallee 1, 21335 Lüneburg, Germany



ARTICLE INFO

Dataset link: <https://doi.org/10.5281/zenodo.10136491>

Keywords:

Multi-layer friction surfacing
Additive manufacturing
Solid state layer deposition
Aluminum

ABSTRACT

Solid-state additive manufacturing (AM) via friction stir based processes is gaining increased attention as these techniques are feasible for several similar and dissimilar material combinations and induce significantly lower energy input to the substrate than fusion-based approaches as material melting is avoided. Available research concentrates on linear depositions; however, further development of these techniques towards application necessitates more complex deposition paths, e.g. curves and the crossing of edges of previously deposited layers. In this study, the solid-state layer deposition process of friction surfacing (FS) is investigated in terms of process behavior and appearance of the resulting deposit when curved deposition paths are applied. With advancing side on the curve's inner edge, material build-up occurs predominantly on this side of the layer, which results in a deposit of inhomogeneous thickness. This phenomenon is related to the FS process characteristic due to the superposition of rotational and travel movement on a curvature, and is more pronounced for curves with small radii. A further challenge exists for closed structures, where the deposition has to cross previously deposited layers. This can be successfully achieved by reducing the travel speed prior to passing the edge to provide sufficient plasticized material thickness below the stud tip. Overall, the study provides an understanding of the FS process behavior and process parameters for curved paths. Furthermore, recommendations for process control and path planning, e.g. for building closed cylindrical shell structures, are deduced.

1. Introduction

Common additive manufacturing (AM) techniques are based on melting a consumable material, e.g. a wire or powder, via an induced energy input, i.e. a laser beam or electric arc. This material solidifies and a structure can be built layer by layer. The approach of AM offers possibilities in design, which are hardly achievable by subtractive approaches, at minimum waste of material [1]. Several metallic materials can be processed with fusion-based AM processes, as presented in the review by Herzog et al. [2]. Despite the strong advantages of AM in general, fusion-based approaches face some challenges, which can mostly be related to the high temperatures that have to be induced in order to melt the material. For instance, porosity formation, hot cracking or heterogeneous microstructures consisting of strongly oriented columnar grains can occur in additively manufactured aluminum structures [3]. Porosity is often formed in the inter-layer regions, i.e. between subsequent layers, resulting in anisotropic behavior of the built structure [4].

Additionally, the strong thermal gradients within the structure might lead to hot cracking [5], significant residual stresses and distortion [6].

Solid-state AM approaches do not necessitate material melting; for instance, friction-stir based AM processes enable the deposition of a consumable material via friction and severe plastic deformation (SPD). The friction stir-based AM techniques are suitable to process a wide range of materials and several similar and dissimilar material combinations can be processed [7]. There are different friction stir-based solid-state AM technologies developed, such as friction stir additive manufacturing (FSAM), additive friction stir deposition (AFSD) or friction surfacing (FS).

The approach of FSAM is close to the friction stir welding (FSW) technique, as a non consumable tool is used to join plates on top of each other. The rotating tool is pressed onto the plate material leading to frictional heat and plasticizing of the plate material, which flows around the tool. The rotating tool is traversed along a path to generate the joint. The technique allows to join multiple sheets on top of each

* Corresponding author.

E-mail address: zina.kallien@hereon.de (Z. Kallien).

other, where different sheet thicknesses or different materials are possible. The joint represents FSW-characteristic areas, i.e. a fine-grained recrystallized structure (stir zone) in the center, a thermo-mechanically affected zone, heat-affected zone and the remaining base material at the outside [8]. The outer parts of the plates are not joined and are commonly removed by post-processing [7].

In contrast, AFSD presents a technique of depositing a consumable material on a substrate using a hollow tool [9]. This tool is positioned above the substrate at a defined gap and experiences a rotational speed. The rotating consumable material is fed through the tool and achieves contact to the substrate surface, where frictional heat is generated and plastic deformation of the consumable material occurs. The consumable material is subsequently fed and fills the small gap between substrate surface and tool with plasticized consumable material. A relative translational movement enables the deposition of the consumable material on the substrate as a layer with a defined thickness, i.e. the height of the gap between tool and substrate surface. AFSD can process different consumable materials like rod, powder or chip material, which enables the technique of AFSD as approach for recycling [10]. The AFSD-deposited material presents an overall refined microstructure [11].

The technique of FS finds potential application as coating [12] or repair [13] technique and is another feasible candidate for solid-state AM [14]. There is a growing research interest in the FS process [15], which is in focus of the present work. In contrast to AFSD and FSAM, FS does not require a tool, which avoids additional phenomena e.g. related to tool wear or contamination. Additionally, the simple setup makes the principle attractive as it can be performed using conventional milling machines [16]. For FS, a rotating stud as a consumable material is pressed onto a substrate, leading to frictional heat and results in the deformation and plasticization of the stud material. A relative movement between substrate and plasticized consumable stud enables the layer deposition. The feasibility of multi-layer FS structures has been demonstrated for steel [17] and aluminum [18] as well as for dissimilar combinations like aluminum on steel [19]. The layers characteristically show a fine-grained microstructure enabled by recrystallization and in terms of tensile strength, the properties of the deposited structures are comparable to the consumable stud base material and no significant directional dependency in terms of tensile strength [20] or detrimental role of layer interfaces has been reported [21]. The FS process offers the possibility to deposit different materials within a multi-layer friction surfacing (MLFS) structure [22] and therefore allows tailored gradients within a structure. Different variants of the FS process were developed, i.e. lateral FS, as presented by Seidi et al. [23], where the significant difference compared to conventional FS is that the material is deposited from the radial surface of the consumable stud creating a thin coating. Similar to conventional FS, lateral FS is also not limited to single layers [24].

Deposition along curved paths is also a relevant topic for fusion-based processes to reduce possible stair-stepping effects [25]. The available research on MLFS is limited to the deposition of linear structures

and especially for the deposition of aluminum alloys, previous works extensively investigated microstructure and mechanical properties of the deposits. However, in order to manufacture more complex parts, the FS process behavior on curves needs to be understood. Therefore, the present work aims to provide the basic knowledge on FS layer deposition on curved paths and has been devised to understand process and deposit characteristics, which is also demonstrated for a MLFS structure. For building closed structures, the challenges of FS deposition across steps is discussed. Finally, the knowledge gained is used to successfully build a closed cylindrical shell structure via FS. Overall, the presented results provide advice for FS layer deposition on curved paths, which is the basis for future development of this process towards more complex AM structures.

2. Materials and methods

The FS experiments are performed using a custom-designed friction welding equipment (RAS, Henry Loitz Robotik, Germany), specialized for solid state layer deposition. The deposition path is programmed via computer numerical control (CNC), which allows free design of the path geometry. The materials used for the experiments are AA5083-H112 as consumable stud material (125 mm length, 20 mm diameter) and AA2050-T84 as substrate (300 mm length, 130 mm width, 12.5 mm thickness). An AA2024 backing plate (300 mm length, 130 mm width, 8 mm thickness) was added between substrate and machine table. The experiments of this study were performed force-controlled and the main FS process parameters are rotational speed, axial force and travel speed. The chosen process parameters are taken from a previous publication [26], leading to suitable depositions. As this study aims for an in-depth analysis of the process behavior on curves, two different curve radii are investigated for single layer FS depositions, where the deposition is always performed along right-hand curves. Linear depositions were performed for reference. Additionally, the direction of the stud rotation (clockwise (CW) or counter-clockwise (CCW)) was varied in order to investigate a possible influence for different curve radii as well as FS process parameters. For the same trajectory and direction of the stud's translational movement, changing the direction of rotation results in a switch of advancing side (AS) and retreating side (RS) in the FS process. The generation of an AS and RS lies in the nature of the FS deposition process where a translational movement is superimposed to the stud's rotational movement. The AS is defined as the side, where rotational and translational movement are in the same direction, where, on the other side, the RS, the rotational movement is in the opposite direction to the translational movement. An overview of all experiments is given in Table 1.

The deposited layers were investigated using a 3D-profilometer (VR-5000, Keyence, Germany) in terms of height profile of the structure. One set of process parameters is selected to demonstrate the building of a MLFS structure on a curved path. In order to build closed structures, the FS process behavior on edges is investigated and discussed. Finally,

Table 1
Overview of applied FS process parameters and direction of rotation on right-hand curves with radius 20 mm and 27.5 mm.

No.	axial force [kN]	rotational speed [rpm]	travel speed [mm/s]	rotation direction	curve radius [mm]
1	8	1200	6	⌚ (CW)	-
2	8	800	4	⌚ (CW)	-
3	8	1200	6	⌚ (CW)	27.5
4	8	1200	6	⌚ (CCW)	
5	8	800	4	⌚ (CW)	
6	8	800	4	⌚ (CCW)	
7	8	1200	6	⌚ (CW)	
8	8	1200	6	⌚ (CCW)	
9	8	800	4	⌚ (CW)	20.0
10	8	800	4	⌚ (CCW)	

the obtained knowledge is used for an application-oriented process by building a closed cylindrical shell structure via MLFS as an exemplary demonstrator for solid state AM.

3. Results and discussion

3.1. FS process behavior on curves

It is well known that the FS process parameters significantly affect the geometry of the deposit, i.e. height and width [27,28]. For the two process parameter sets used in this study, linear depositions have been performed for reference, Fig. 1. The slower rotational and travel speed,

i.e. 800 rpm and 4 mm/s, respectively, lead to significantly thicker layers. Both deposits show the FS-characteristic rough surface presenting a circular pattern. Except for the start and end of the layer, i.e. the areas where the process has been initiated or the stud has been retracted, the deposits present a homogeneous thickness along deposition length as well along its width, Fig. 1. The obtained layer thicknesses are 1.4 mm (8 kN, 1200 rpm, 6 mm/s) and 2.9 mm (8 kN, 800 rpm, 4 mm/s), respectively.

The deposited semi circle paths are presented in Figs. 2 and 3 for both process parameter sets investigated. The deposit thickness is comparable to the linear reference deposition. The thinner deposition, Fig. 2, presents a homogeneous thickness; however, for a smaller curve

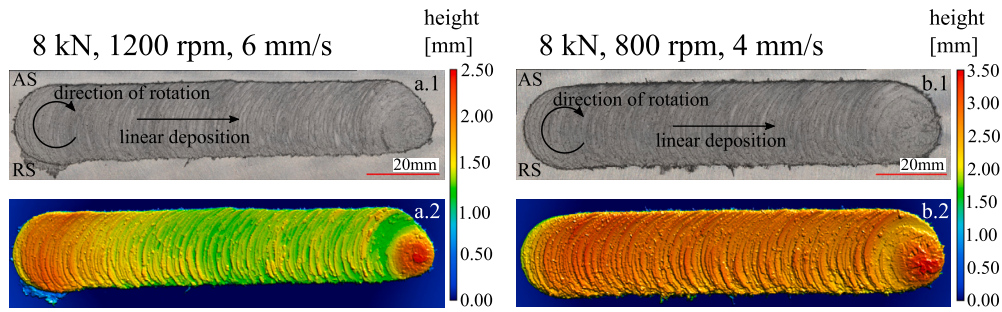


Fig. 1. Appearance and layer height mapping of linear deposition at different process parameters, i.e. process No. 1 (a.1, a.2) and No.2 (b.1, b.2).

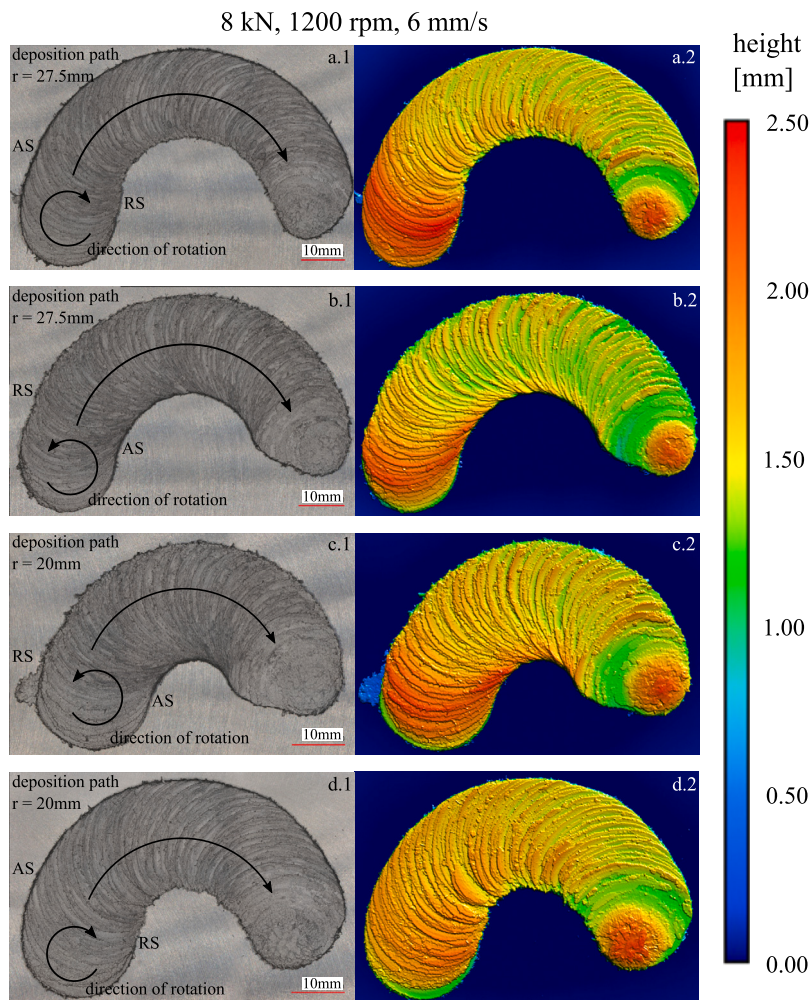


Fig. 2. Appearance and layer height mapping of semi circle FS deposits (8 kN, 1200 rpm, 6 mm/s) for curve radius of 27.5 mm, i.e. process No. 3 (a.1, a.2) and No.4 (b.1, b.2), and 20 mm, i.e. process No. 8 (c.1, c.2) and No. 7 (d.1, d.2).

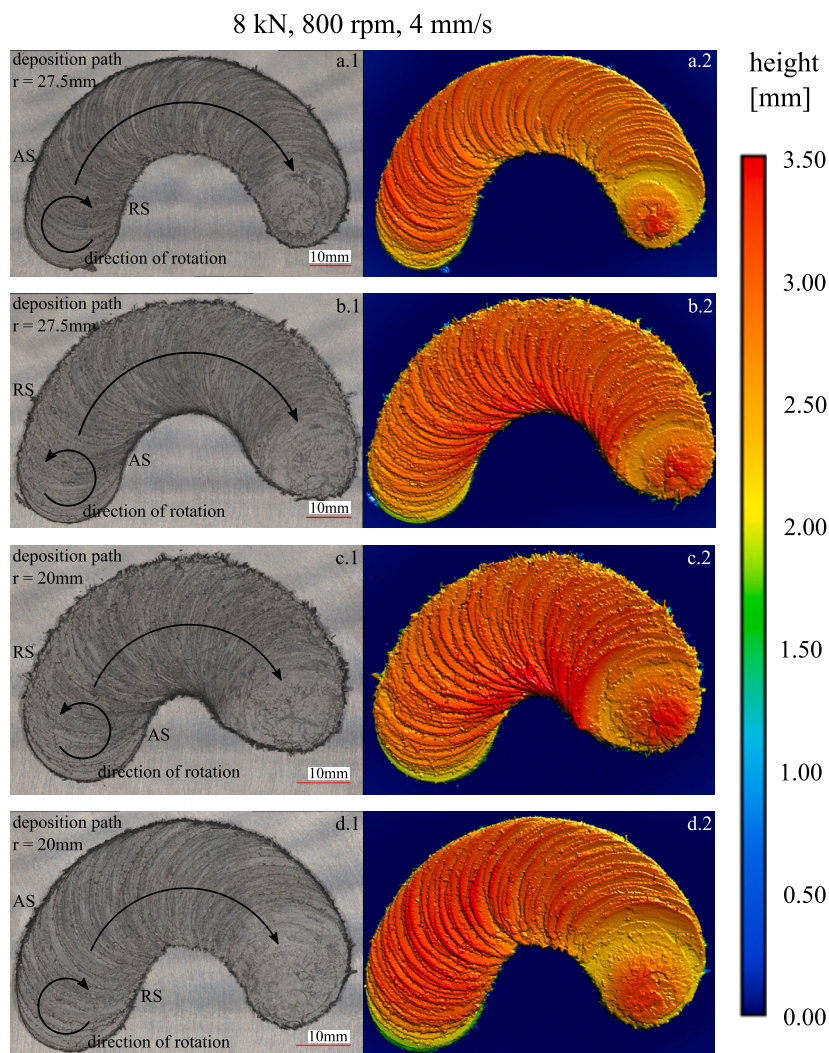


Fig. 3. Appearance and layer height mapping of semi circle FS deposits (8 kN, 800 rpm, 4 mm/s) for curve radius of 27.5 mm, i.e. process No. 5 (a.1, a.2) and No. 6 (b.1, b.2), and 20 mm, i.e. process No. 10 (c.1, c.2) and No. 9 (d.1, d.2).

radius of 20 mm, the material tends to build up at the inner edge, especially for the process with counter-clockwise rotation of the stud, Fig. 2, i.e. when the retreating side is at the outer edge of the deposition path. For the thicker layers achieved by 8 kN, 800 rpm, 4 mm/s, Fig. 3, the observed phenomenon is even more pronounced. For a quantitative assessment, the height profiles of the deposits were analyzed after half of the welding path from outer to inner edge, Fig. 4. The profiles show that all depositions using constant process parameters present similar layer thickness, including the results for the linear deposits. As mentioned above, the only deviation in the layer thickness is determined at the retreating side for the curved deposits performed with CCW stud rotation. This can also be observed from the corresponding cross sections, Figs. 5 and 6. The effect is most pronounced when parameters for thick layers and the smaller curve radius are used, resulting in up to 1 mm height difference between inner and outer part of the deposit.

The explanation for this deposition behavior can be found in the characteristic of the FS process. During initial plasticizing, when no travel speed is applied, the relative velocity of advancing and retreating side is symmetric, Fig. 7(a).

The superposition of a relative translational movement at a defined travel speed to the rotating stud results in the asymmetric distribution of relative velocity, i.e. the relative velocity differs between advancing and retreating side, Fig. 7(b), [29]. Therefore, compared to the initial position, the nil relative velocity center is shifted to the retreating side,

where rotational speed applies velocity in the opposite direction than the direction of travel speed. The magnitude of this shift depends on the rotational and travel speed [29] as well as stud length and material stiffness affecting the displacement response to the deflecting force resulting from the described asymmetric conditions. The stud tends to shift to the advancing side for linear deposition paths [30], see Fig. 7(c). A curved deposition path results in different travel speeds across the deposition path, i.e. slower at the inner edge and faster at the outer edge. When the advancing side (applied rotational velocity in the same direction as travel speed) is on the inner side, it covers a shorter distance than the retreating side (applied rotational velocity opposite direction as travel speed), intensifying the asymmetry between both sides. This results in material build up at the inner curve edge for this configuration. In order to achieve a homogeneous FS layer deposition on curved structures, especially for small curve diameters and/or thick layer geometries, the process setup and path design should be planned accordingly, i.e. advancing side at the outer edge.

The process feasibility on curved deposition paths was also investigated in terms of MLFS structures. The deposition of multiple layers on top of each other was performed with a curve radius of 27.5 mm at CW stud rotation, building an open cylindrical shell structure from layers deposited at 288° circular sections. The structure is presented in Fig. 8. With the presented setup, the FS principle showed a robust and reliable process behavior on a curved deposition path for a structure of 25

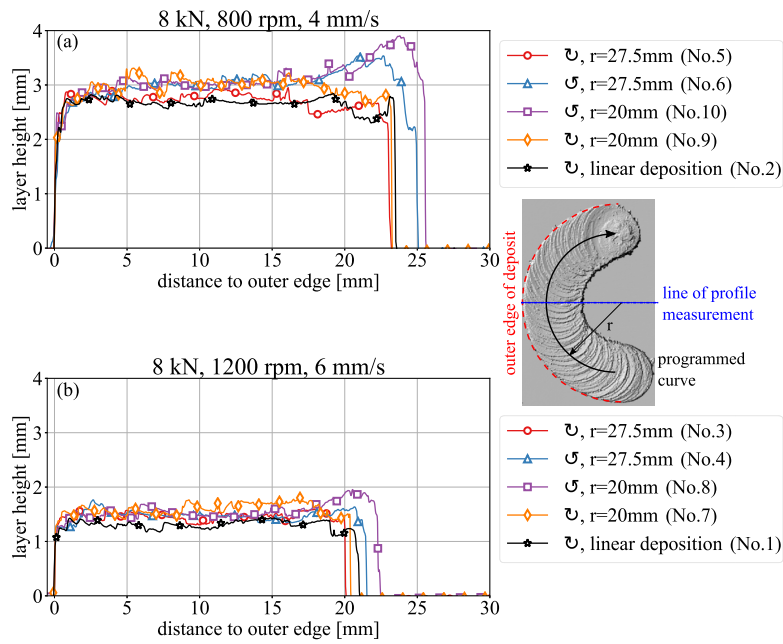


Fig. 4. Height profiles for circular FS deposits at two different radii (20 mm and 27.5 mm) for two different process parameter sets, i.e. (a) 8 kN/800 rpm/4 mm/s and (b) 8 kN/1200 rpm/6 mm/s, where the height profile was taken after 1/4 circle. Height profiles for corresponding linear deposits are included for reference.

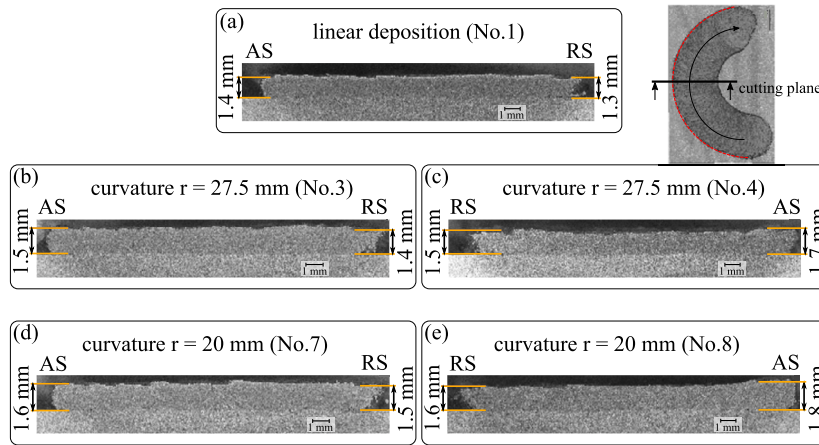


Fig. 5. Cross sections taken after quarter circle single layer depositions at 8 kN, 1200 rpm and 6 mm/s. The outer edge of the deposit is on the left.

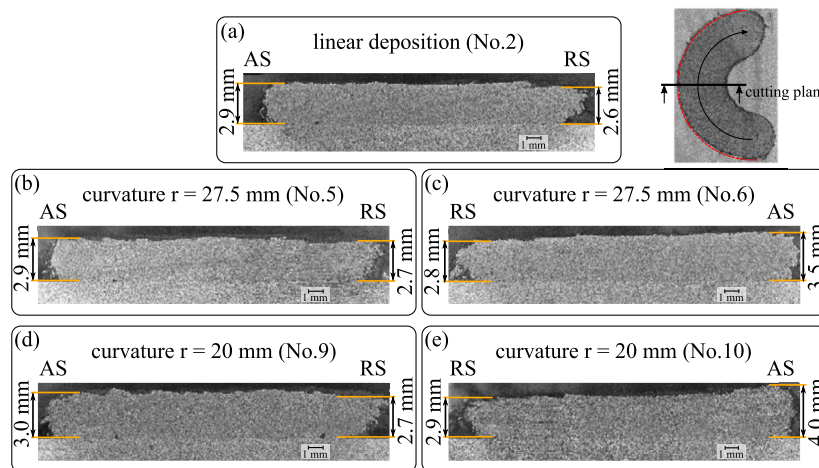


Fig. 6. Cross sections taken after quarter circle single layer depositions at 8 kN, 800 rpm and 4 mm/s. The outer edge of the deposit is on the left.

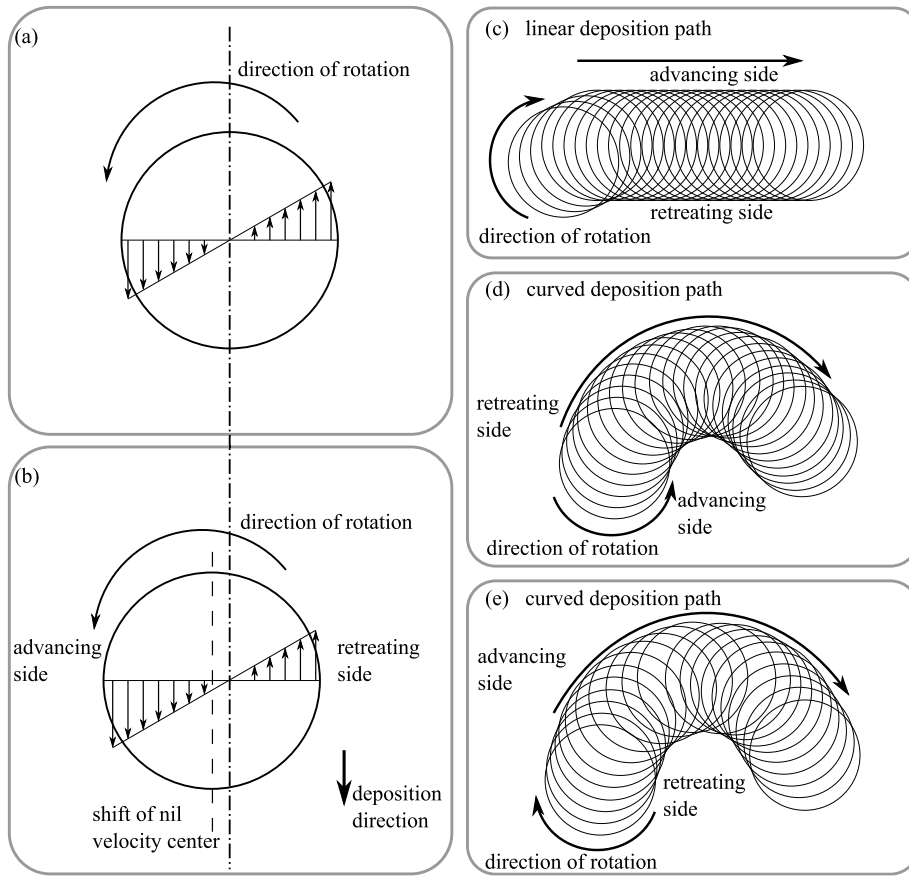


Fig. 7. Schematic of velocity distribution for (a) a rotating stud, which is the case during FS plasticizing, and (b) rotating stud with superimposed relative translational movement at a defined travel speed during layer deposition, which leads to asymmetric velocity distribution [29]. This process characteristic leads to a tendency of the deposition towards the advancing side, which is shown for a linear deposition path (c). On curved deposition paths, advancing side on the inner edge of the path (d) can lead to a material build-up at the inner edge resulting in an inhomogeneous layer thickness, where advancing side at the outer edge of the path (e) can lead to a more homogeneous thickness.

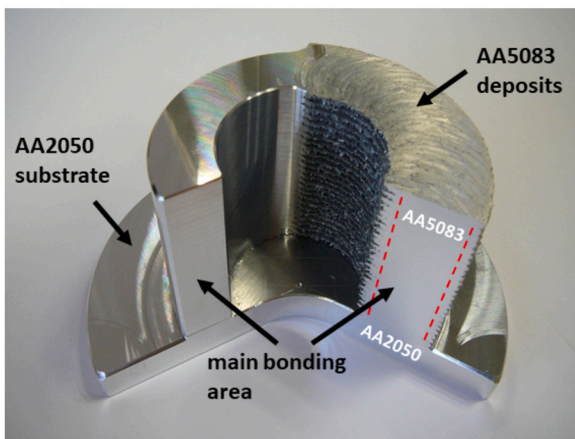


Fig. 8. Open cylindrical shell structure from AA5083 MLFS layers on AA2050 substrate; partial machining of the structure revealed that approx. 80% of the deposited material forms the defect-free structural bulk material indicated by the red dashed lines.

layers. After building the MLFS structure, partial machining was performed in order to remove the FS-characteristic rough surfaces. For the FS process conditions and materials used, the remaining defect-free volume after machining represents approx. 80% of the overall deposited volume.

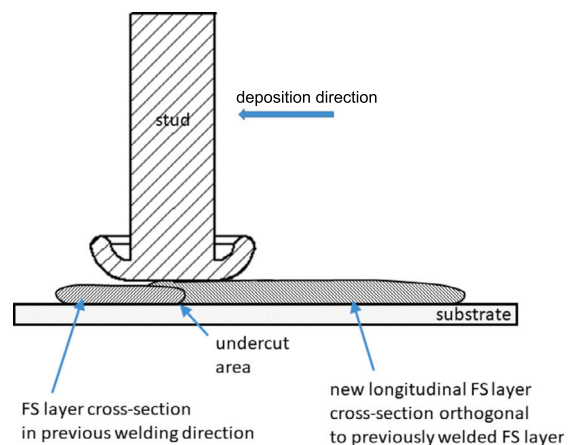


Fig. 9. Schematic longitudinal section of FS layer crossing previous deposit. The successful deposition can be achieved by providing enough plasticized material below the stud in order to create a defect-free bonding.

3.2. MLFS across edges

In order to build closed structures, the deposition has to cross previously deposited layers, Fig. 9. The solution is to provide enough plasticized material below the stud to bridge the gap that is formed during stud lift/step-up, avoiding volumetric defects. If not enough plasticized material is provided, this would lead to a collision of the non-plasticized

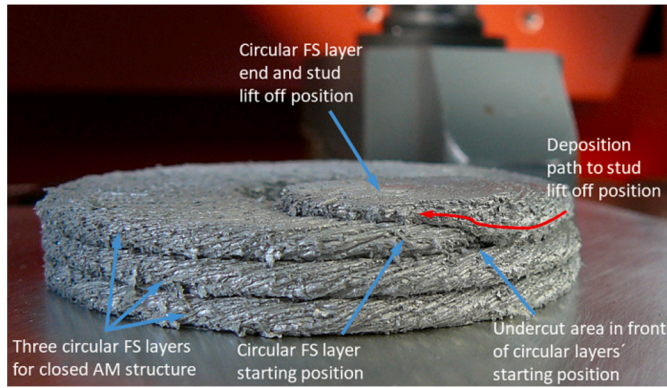


Fig. 10. Crossing of a step in order to build a closed cylindrical shell structure.

stud material with the edge of the previous deposit, potentially leading to process instability or even failure. The successful and stable crossing of an edge can be ensured by reducing the travel speed before crossing an edge in order to provide sufficient time for the rotating stud to safely deposit material across the edge, Fig. 10.

In the work of Soujon et al. [18], the investigation of edge angle for the FS layer deposition showed that a surface with increasing angle leads to less pronounced formation of an upper and a lower part of the plasticized material, causing a more balanced force distribution at the stud tip. This is also assumed for building closed structures, i.e. the machining of the edge would help to ensure process stability and successful deposition of the subsequent layer. However, machining of the respective edges would lead to an overall higher effort for building the structure, therefore, an adaptive process control, i.e. local adjustment of the process parameters, is preferred.

In case of defects, which might occur especially in the areas where layers cross previous depositions, post-processing might be necessary. For MLFS structures, Soujon et al. [18] investigated the effect of post-processing via hybrid friction diffusion bonding (HFDB) on the defect volume. HFDB is a solid state technique that uses a pin-less tool to process a subsequent structure at defined tool rotational speed, applied axial force and travel speed. It was shown that HFDB is a promising post-processing approach to consolidate defects resulting in almost defect-free interfaces for various FS conditions for overlapping layers [18].

Overall, the obtained findings present a feasible strategy for successfully building closed and more complex structures via MLFS. Previous studies mentioned above, see for instance [20,26], extensively investigated microstructural and mechanical properties. Although these investigations have been performed for linear deposition, the curved deposition path did not change the overall nature of the FS layer deposition, i.e. in terms of microstructure evolution no obvious changes have been detected and, similar to linear deposition, defect-free bond-

ing could be observed between layer and substrate as well as between the layers. The strategy is applied to a possible test case application in the following.

4. Test case: application of the approach for building a closed structure from AA6082

The test case aims to additively build a closed cylinder shell structure, i.e. piston, via MLFS. For forged pistons, both high and low silicon aluminum alloys are used, with hardness, ductility and in particular thermal expansion tailored to the specific needs. For this application scenario extruded AA6082, typically used in T6 temper for subtractively machined pistons, is selected for its widespread use in high stress applications [31] and in order to extend the gained knowledge onto another aluminum alloy. In this particular scenario, the piston structure could benefit from a refined, forge-like microstructure as well as the potential combination of dissimilar alloys to selectively adapt piston sections to different compressive loads and thermal stresses while reducing part weight.

The cylindrical shell structure with a radius of 20 mm was built at constant process parameters of 7 kN, 2000 rpm and 12 mm/s, which are process parameters also used by Hanke and dos Santos [32] for AA6082 consumable stud material. Every single layer performed a full 360° circle and the starting points of the layers were chosen with 90° offset to the previous one. The advancing side was chosen to be at the outer edge of the curvature. At the edges, i.e. when crossing the previous layer, the travel speed was reduced to 10 mm/s. The structure was built on a AA6082 substrate and is presented in Fig. 11. After machining to the final structure, a sound and visually defect-free piston structure from MLFS deposited AA6082 is obtained.

The successful build of a piston structure highlights the robustness of the FS principle. However, machining is necessary to achieve a good surface quality. For large-scale structures, the discontinuity of the process, where achievable deposit geometry are mainly limited by the stud dimensions, remains a challenge because many layers are necessary and post-processing might be required at the layer interfaces to ensure defect-free bonding. Overall, the MLFS solid state AM approach is suitable for parts with a strong need for homogeneity. Furthermore, MLFS is a considerable approach especially for temperature sensitive structures due to the low heat input.

5. Conclusion

In the present study, necessary elements to build a closed cylinder shell structure in solid state via MLFS were investigated. The process behavior on curves and across edges has been analyzed and discussed and the proof of the feasibility has been demonstrated successfully. In order to build complex MLFS structures, e.g. with curved deposition paths, the following conclusions can be drawn:

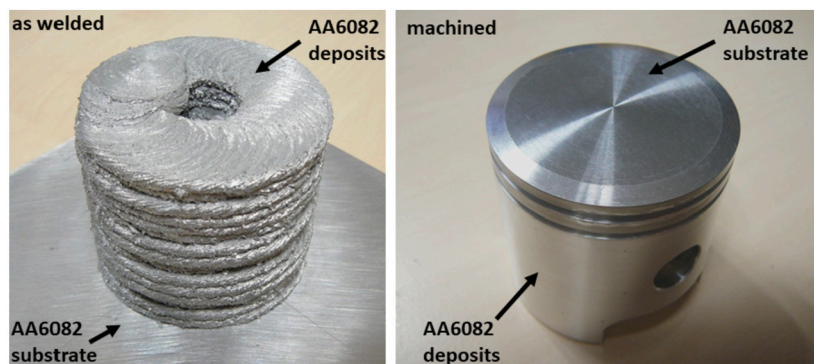


Fig. 11. Closed cylindrical shell structure from AA6082 additively manufactured via MLFS: as welded (left) and after machining to the final piston (right).

- Solid state layer deposition via the FS principle is very robust not only on linear but also on curved deposition paths for single layers as well as MLFS stacks.
- The advancing side at the outer edge of the curvature is advantageous for a homogeneous deposition thickness, especially for small curve radii and/or thick FS layers.
- To ensure a successful deposition across edges, the adaption of process parameters can be helpful.
- Post-processing in order to remove the FS-characteristic rough parts of the layers of the build structure is probably necessary for most applications. Furthermore, additional post-processing strategies might be required to optimize e.g. in terms of geometry or properties. For the setup and parameters used in this study approx. 80% of the deposited material remained after machining to the final geometry.

CRedit authorship contribution statement

Zina Kallien: Conceptualization, Data curation, Formal analysis, Investigation, Methodology, Validation, Visualization, Writing – original draft, Writing – review & editing. **Lars Rath:** Investigation, Methodology, Writing – review & editing. **Arne Roos:** Supervision, Writing – review & editing. **Benjamin Klusemann:** Funding acquisition, Resources, Supervision, Writing – review & editing.

Declaration of competing interest

The authors declare that they have no known competing financial interests or personal relationships that could have appeared to influence the work reported in this paper.

Data availability

The obtained data of this research is online available at Zenodo (<https://doi.org/10.5281/zenodo.10136491>).

Funding

This project has received funding from the European Research Council (ERC) under the European Unions Horizon 2020 research and innovation programme (grant agreement No 101001567).

References

- [1] S. Ford, M. Despeisse, Additive manufacturing and sustainability: an exploratory study of the advantages and challenges, *J. Clean. Prod.* 137 (2016) 1573–1587.
- [2] D. Herzog, V. Seyda, E. Wycisk, C. Emmelmann, Additive manufacturing of metals, *Acta Mater.* 117 (2016) 371–392.
- [3] O. Abdulhameed, A. Al-Ahmari, W. Ameen, S.H. Mian, Additive manufacturing: challenges, trends, and applications, *Adv. Mech. Eng.* 11 (2) (2019) 1687814018822880.
- [4] J. Bai, H. Ding, J. Gu, X. Wang, H. Qiu, Porosity Evolution in Additively Manufactured Aluminium Alloy During High Temperature Exposure, *IOP Conference Series: Materials Science and Engineering*, vol. 167, IOP Publishing, 2017, p. 012045.
- [5] E. Cicalà, G. Duffet, H. Andrzejewski, D. Grevey, S. Ignat, Hot cracking in Al-Mg-Si alloy laser welding - operating parameters and their effects, *Mater. Sci. Eng. A* 395 (1–2) (2005) 1–9.
- [6] C. Li, Z. Liu, X. Fang, Y. Guo, Residual stress in metal additive manufacturing, *Proc. CIRP* 71 (2018) 348–353.
- [7] R.S. Mishra, R.S. Haridas, P. Agrawal, Friction stir-based additive manufacturing, *Sci. Technol. Weld. Join.* 27 (3) (2022) 141–165, <https://doi.org/10.1080/13621718.2022.2027663>.
- [8] C. Genevois, A. Deschamps, A. Denquin, B. Doisneau-Cottignies, Quantitative investigation of precipitation and mechanical behaviour for AA2024 friction stir welds, *Acta Mater.* 53 (8) (2005) 2447–2458.
- [9] K. Kandasamy, Solid state joining using additive friction stir processing, US Patent 9,511,445 (Dec. 6 2016).
- [10] S. Beck, C. Williamson, R. Kinser, B. Rutherford, M. Williams, B. Phillips, P. Allison, J. Jordon, Examination of microstructure and mechanical properties of direct additive recycling for Al-Mg-Mn alloy machine chip waste, *Mater. Des.* (2023) 111733.
- [11] D.Z. Avery, C. Cleek, B.J. Phillips, M. Rekha, R.P. Kinser, H. Rao, L. Brewer, P. Allison, J. Jordon, Evaluation of microstructure and mechanical properties of Al-Zn-Mg-Cu alloy repaired via additive friction stir deposition, *J. Eng. Mater. Technol.* 144 (3) (2022) 031003.
- [12] M. Yu, H. Zhao, Z. Zhang, L. Zhou, X. Song, N. Ma, Texture evolution and corrosion behavior of the AA6061 coating deposited by friction surfacing, *J. Mater. Process. Technol.* 291 (2020) 117005, <https://doi.org/10.1016/j.jmatprotec.2020.117005>.
- [13] R. Damodaram, P. Rai, S. Cyril Joseph Daniel, R. Bauri, D. Yadav, Friction surfacing: a tool for surface crack repair, *Surf. Coat. Technol.* 422 (2021) 127482, <https://doi.org/10.1016/j.surfcoat.2021.127482>.
- [14] J.J.S. Dilip, G.D. Janaki Ram, B.E. Stucker, Additive manufacturing with friction welding and friction deposition processes, *Int. J. Rapid Manuf.* 3 (1) (2012) 56–69.
- [15] E. Seidi, S.F. Miller, B.E. Carlson, Friction surfacing deposition by consumable tools, *J. Manuf. Sci. Eng.* 143 (12) (2021) 031012, <https://doi.org/10.1115/1.4050924>.
- [16] J.C. Galvis, P. Oliveira, M.F. Hupalo, J.P. Martins, A. Carvalho, Influence of friction surfacing process parameters to deposit AA6351-T6 over AA5052-H32 using conventional milling machine, *J. Mater. Process. Technol.* 245 (2017) 91–105, <https://doi.org/10.1016/j.jmatprotec.2017.02.016>.
- [17] J.J.S. Dilip, S. Babu, S.V. Rajan, K.H. Rafi, G.D. Janaki Ram, B.E. Stucker, Use of friction surfacing for additive manufacturing, *Mater. Manuf. Process.* 28 (2) (2013) 189–194, <https://doi.org/10.1080/10426914.2012.677912>.
- [18] M. Soujoun, Z. Kallien, A. Roos, B. Zeller-Plumhoff, B. Klusemann, Fundamental study of multi-track friction surfacing deposits for dissimilar aluminum alloys with application to additive manufacturing, *Mater. Des.* 219 (5) (2022) 110786, <https://doi.org/10.1016/j.matdes.2022.110786>.
- [19] E.S. Abdelall, A.F. Al-Dwairi, S.M. Al-Raba'a, M. Eldakrouy, Printing functional metallic 3d parts using a hybrid friction-surfacing additive manufacturing process, *Prog. Addit. Manuf.* 10 (3) (2021) 103, <https://doi.org/10.1007/s40964-021-00193-3>.
- [20] L. Rath, Z. Kallien, A. Roos, J.F.d. Santos, B. Klusemann, Anisotropy and mechanical properties of dissimilar al additive manufactured structures generated by multi-layer friction surfacing, *Int. J. Adv. Manuf. Technol.* 117 (6) (2023) 371, <https://doi.org/10.1007/s00170-022-10685-3>.
- [21] Z. Kallien, C. Knothe-Horstmann, B. Klusemann, Fatigue crack propagation in AA5083 structures additively manufactured via multi-layer friction surfacing, *Addit. Manuf. Lett.* 6 (2023) 100154, <https://doi.org/10.1016/j.addlet.2023.100154>.
- [22] S.M. Bararpour, H. Jamshidi Aval, R. Jamaati, Mechanical alloying by friction surfacing process, *Mater. Lett.* 254 (2019) 394–397, <https://doi.org/10.1016/j.matlet.2019.07.113>.
- [23] E. Seidi, S.F. Miller, A novel approach to friction surfacing: experimental analysis of deposition from radial surface of a consumable tool, *Coatings* 10 (11) (2020) 1016, <https://doi.org/10.3390/coatings10111016>.
- [24] E. Seidi, S.F. Miller, Feasibility of multilayer solid-state deposition via lateral friction surfacing for metal additive manufacturing, *J. Mater. Res. Technol.* 1 (1) (2022) 82, <https://doi.org/10.1016/j.jmrt.2022.07.158>.
- [25] S. Cam, E. Gunpinar, Fluid flow-inspired curvature-aware print-paths from hexahedral meshes for additive manufacturing, *Comput. Aided Des.* 159 (2023) 103500, <https://doi.org/10.1016/j.cad.2023.103500>.
- [26] Z. Kallien, M. Hoffmann, A. Roos, B. Klusemann, Correlation of microstructure and local mechanical properties along build direction for multi-layer friction surfacing of aluminum alloys, *JOM*, <https://doi.org/10.1007/s11837-023-06046-4>.
- [27] J. Gandra, H. Krohn, R.M. Miranda, P. Vilaça, L. Quintino, J.F. Dos Santos, Friction surfacing—a review, *J. Mater. Process. Technol.* 214 (5) (2014) 1062–1093, <https://doi.org/10.1016/j.jmatprotec.2013.12.008>.
- [28] M.E. Özcan, The influence of parameters on the evolution of the friction surfacing method - a review, *J. Mech. Sci. Technol.* 36 (2) (2022) 723–730, <https://doi.org/10.1007/s12206-022-0120-z>.
- [29] J. Li, T. Shinoda, Underwater friction surfacing, *Surf. Eng.* 16 (1) (2000) 31–35, <https://doi.org/10.1179/026708400322911483>.
- [30] H. Sakihama, H. Tokisue, K. Katoh, Mechanical properties of friction surfaced 5052 aluminum alloy, *Mater. Trans.* 44 (12) (2003) 2688–2694, <https://doi.org/10.2320/amatrans.44.2688>.
- [31] M.D. Sandar, S. Yasasvi, Design and analysis of aluminium 6082-T6 piston, *Int. J. Innov. Res. Sci. Technol.* 3 (11) (2017) 39–47.
- [32] S. Hanke, J.F. dos Santos, Comparative study of severe plastic deformation at elevated temperatures of two aluminium alloys during friction surfacing, *J. Mater. Process. Technol.* 247 (2017) 257–267, <https://doi.org/10.1016/j.jmatprotec.2017.04.021>.